Electronic Supplementary Material (ESI) for Physical Chemistry Chemical Physics

Supporting Information

Drastic sensitivity enhancement in ^{29}Si MAS NMR in zeolites and mesoporous silica materials by paramagnetic doping of Cu^{2+}

Satoshi Inagaki, Izuru Kawamura, Yukichi Sasaki, Kaname Yoshida, Akira Naito, Yoshihiro Kubota*

Table S1 Textural properties of mesoporous silica materials and zeolite beta

Sample	BET surface area / $m^2\ g^{-1}$	Micropore volume (*t*-plot) / $cm^3\ g^{-1}$	Mesopore volume (BJH) / $cm^3\ g^{-1}$	Mesopore diameter, *D* (BJH) / nm	d_{100} value (XRD) / nm	Thickness of mesopore wall, t^a / nm
MCM-41	1150	$< 10^{-4}$	1.04	2.8	3.48	1.7
SBA-15	1007	0.025	1.16	8.3	9.80	3.0
dealuminated beta	457	0.228	–	–	–	–
pure silica beta	488	0.203	–	–	–	–
[Fe]-beta	560	0.240	–	–	–	–

a The thickness of mesopore wall, *t*, was estimated using the equation (1):

$$t = \frac{2}{\sqrt{3}} d_{100} - D \quad (1)$$

Figure Captions in Supporting Information

Figure S1. Powder XRD patterns of (a) MCM-41 and (b) SBA-15.

Figure S2. Nitrogen adsorption-desorption isotherms at 77 K of (a) MCM-41 and (b) SBA-15. The isotherm of (b) was offset vertically with 800 cm^3 (S.T.P.) g^{-1}. Open and closed symbols mean adsorption and desorption branches, respectively.

Figure S3. Pore size distributions of (a) MCM-41 and (b) SBA-15 determined by the BJH method.

Figure S4. Typical SEM images of (a) MCM-41 and (b) SBA-15.

Figure S5. Peak-area distributions of Q^2, Q^3 and Q^4 signals by various recycle times from 3 to 240 s. (a) Unmodified SBA-15; (b) 1.0-$Cu(NO_3)_2$/SBA-15; (c) 1.0-Cu-EDTA/SBA-15.

Figure S6. Powder XRD patterns of (a) dealuminated beta, (b) pure silica beta and (c) [Fe]-beta (Si/Fe = 58).

Figure S7. Nitrogen adsorption-desorption isotherms at 77 K of (a) dealuminated beta, (b) pure silica beta and (c) [Fe]-beta (Si/Fe = 58). The isotherms of (b) and (c) were offset vertically with 200 and 400 cm^3 (S.T.P.) g^{-1}, respectively. Open and closed symbols mean adsorption and desorption branches, respectively.

Figure S8. Typical SEM images of (a) dealuminated beta, (b) pure silica beta and (c) [Fe]-beta (Si/Fe = 58).

Figures S9. (A) Relative peak heights of Q^4 signals at –112 ppm by various recycle times from 3 to 30 s. (○) Unmodified deAl-beta; (△) 0.1-$Cu(NO_3)_2$/deAl-beta; (◇) 0.3-$Cu(NO_3)_2$/deAl-beta; (□) 0.5-$Cu(NO_3)_2$/deAl-beta; (●) 1.0-$Cu(NO_3)_2$/deAl-beta.

(B) Relative peak heights of Q^4 signals at –115 ppm by various recycle times from 3 to 30 s. (○) Unmodified deAl-beta; (△) 0.1-$Cu(NO_3)_2$/deAl-beta; (◇) 0.3-$Cu(NO_3)_2$/deAl-beta; (□) 0.5-$Cu(NO_3)_2$/deAl-beta; (●) 1.0-$Cu(NO_3)_2$/deAl-beta.

Figure S10. Relative peak heights of Q^4 signals at –112 ppm by various recycle times from 3 to 30 s. (○) unmodified deAl-beta; (△) 1.0-$Co(NO_3)_2$/deAl-beta; (◇) 1.0-$Ni(NO_3)_2$/deAl-beta; (●) 1.0-$Cu(NO_3)_2$/deAl-beta.

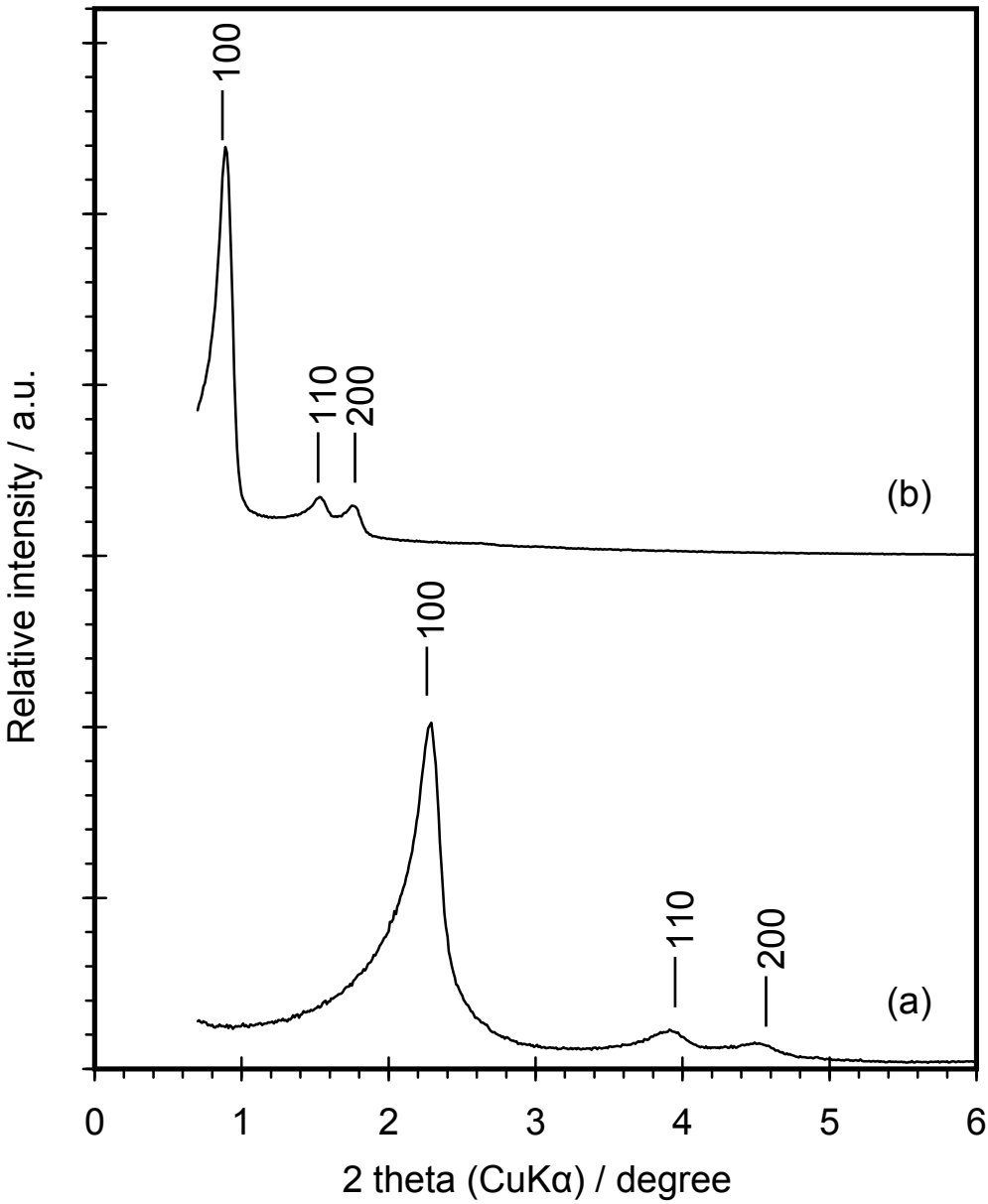

Figure S1. Powder XRD patterns of (a) MCM-41 and (b) SBA-15.

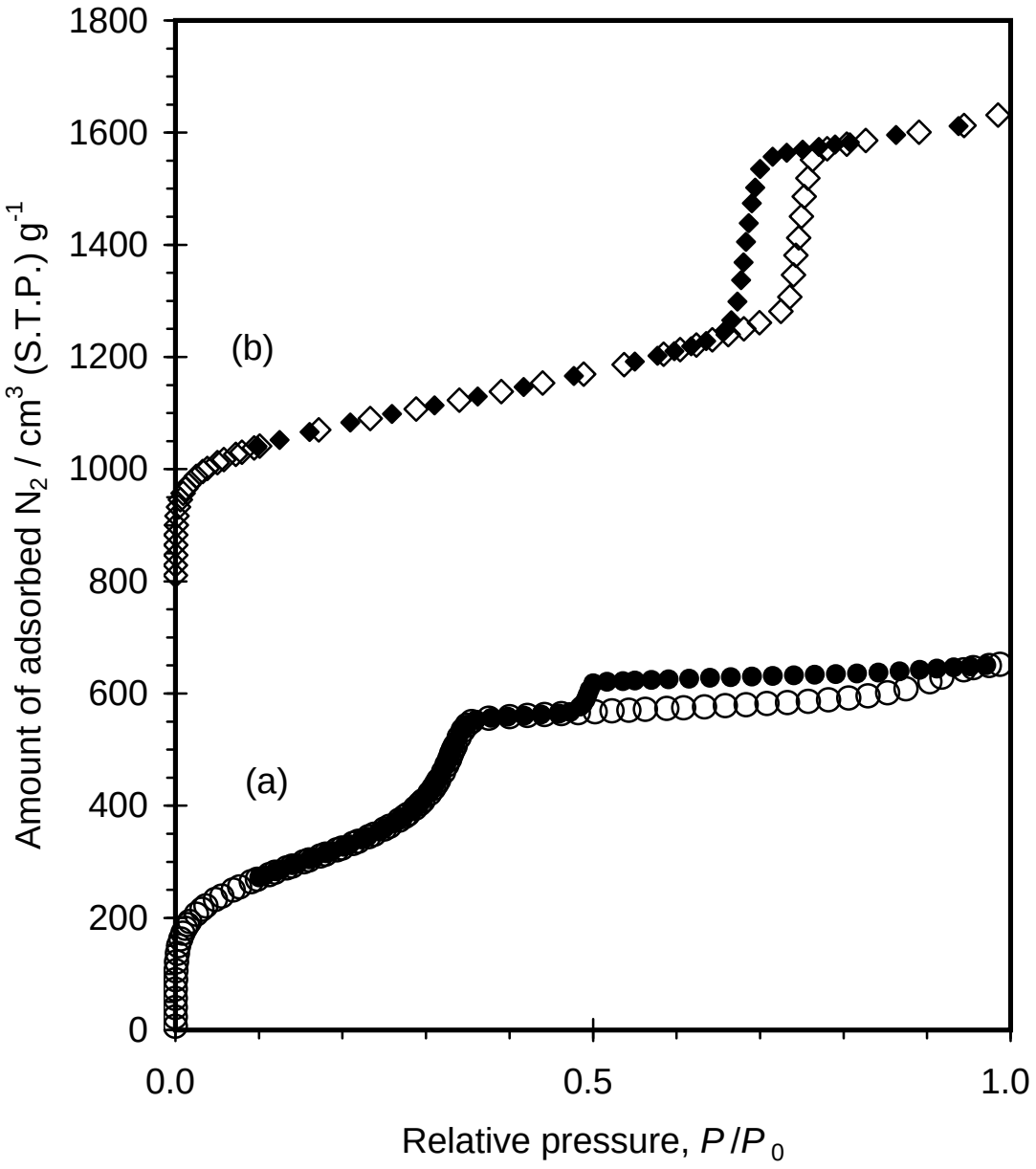

Figure S2. Nitrogen adsorption-desorption isotherms at 77 K of (a) MCM-41 and (b) SBA-15. The isortherm of (b) was offset vertically with 800 cm^3 (S.T.P.) g^{-1}. Open and closed symbols mean adsorption and desorption branches, respectively.

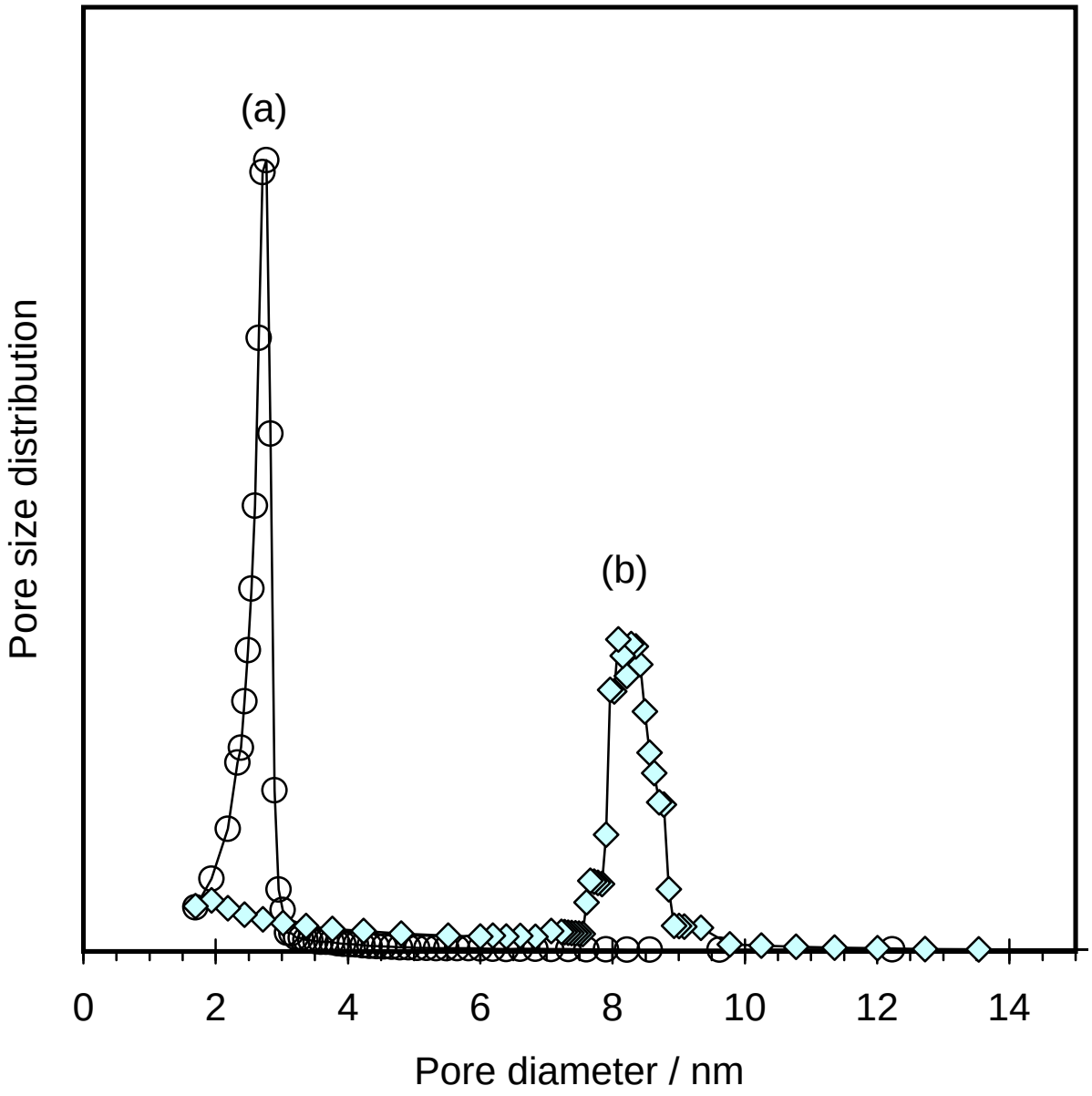

Figure S3. Pore size distributions of (a) MCM-41 and (b) SBA-15 determined by the BJH method.

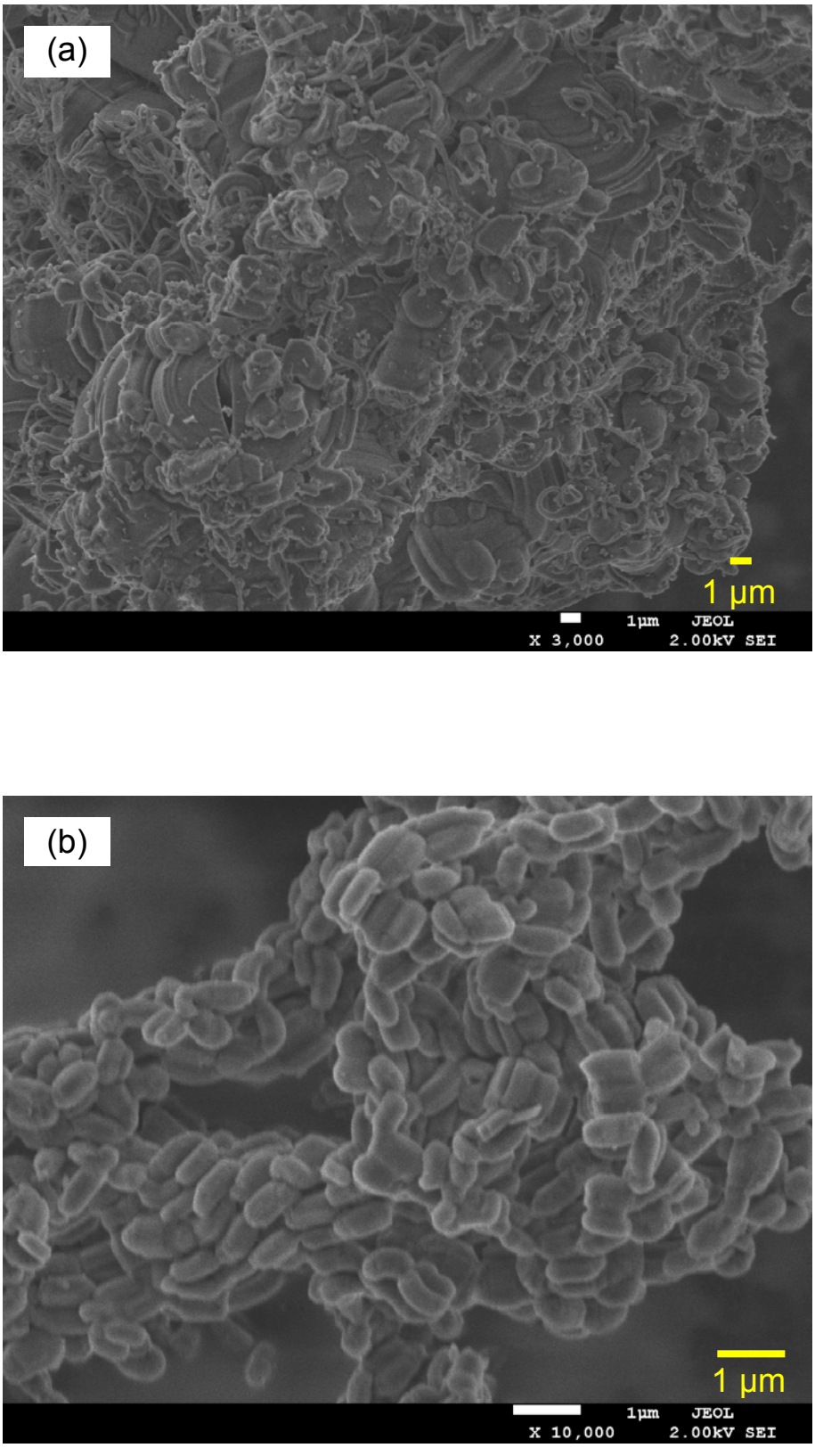

Figure S4. Typical SEM images of (a) MCM-41 and (b) SBA-15.

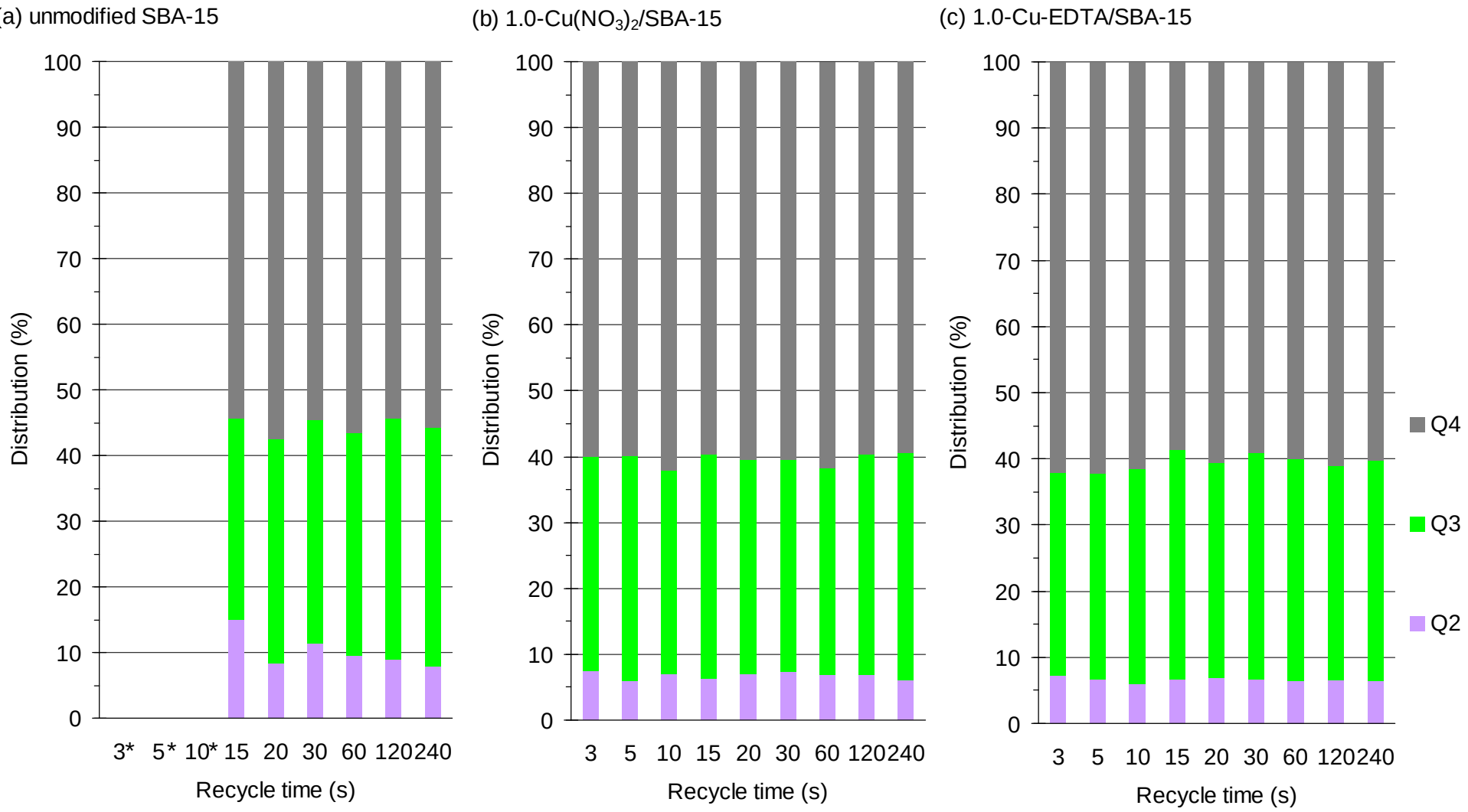

Figure S5. Peak-area distributions of Q^2, Q^3 and Q^4 signals by various recycle times from 3 to 240 s. (a) Unmodified SBA-15; (b) 1.0-Cu$(NO_3)_2$/SBA-15; (c) 1.0-Cu-EDTA/SBA-15.

*The broad spectra of 3, 5 and 10 s (recycle time) in unmodified SBA-15 are impossible to deconvolute as Q^2, Q^3 and Q^4 signals.

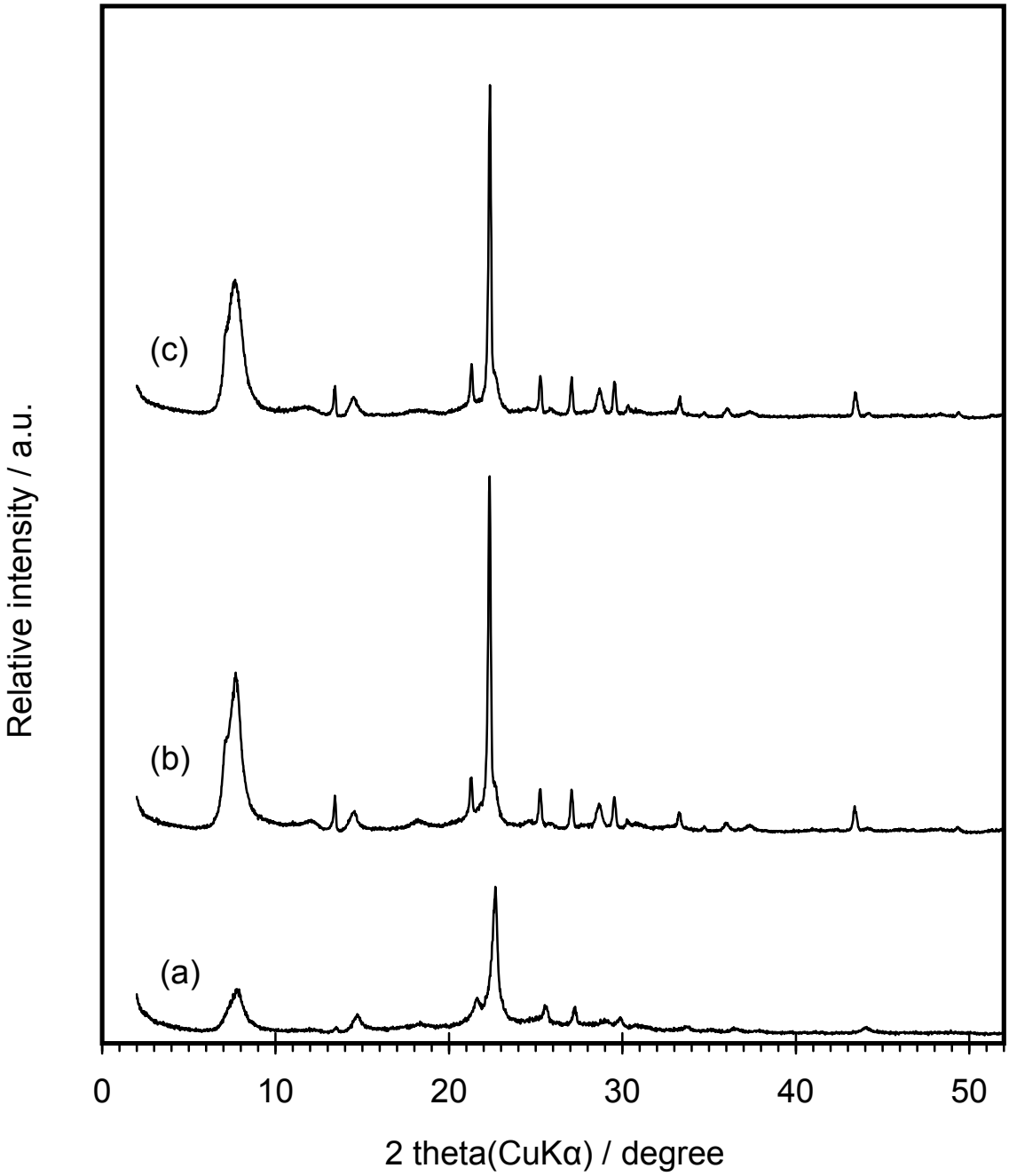

Figure S6. Powder XRD patterns of (a) dealuminated beta, (b) pure silica beta and (c) [Fe]-beta (Si/Fe = 58).

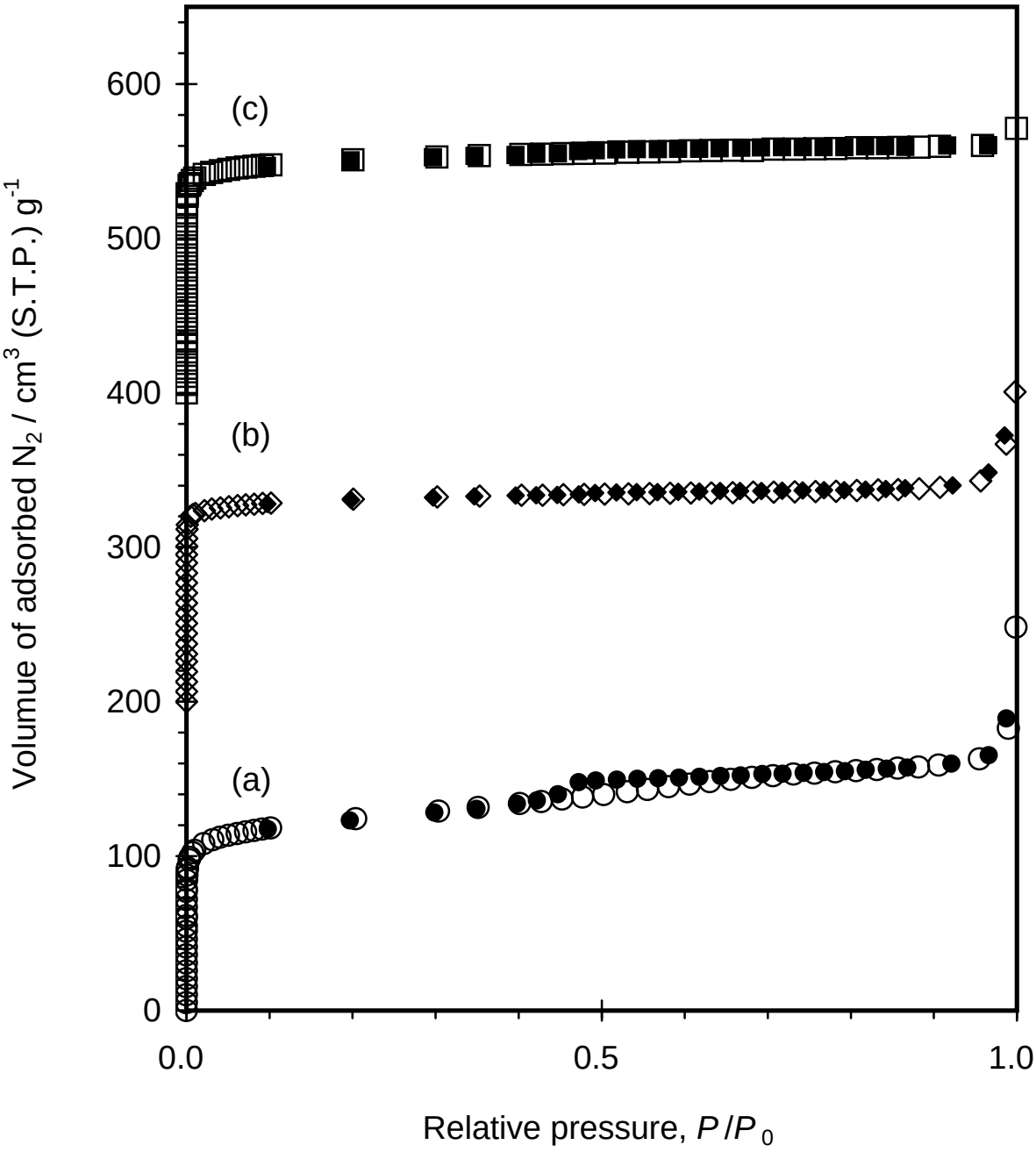

Figure S7. Nitrogen adsorption-desorption isotherms at 77 K of (a) dealuminated beta, (b) pure silica beta and (c) [Fe]-beta (Si/Fe = 58). The isotherms of (b) and (c) were offset vertically with 200 and 400 cm^3 (S.T.P.) g^{-1}, respectively. Open and closed symbols mean adsorption and desorption branches, respectively.

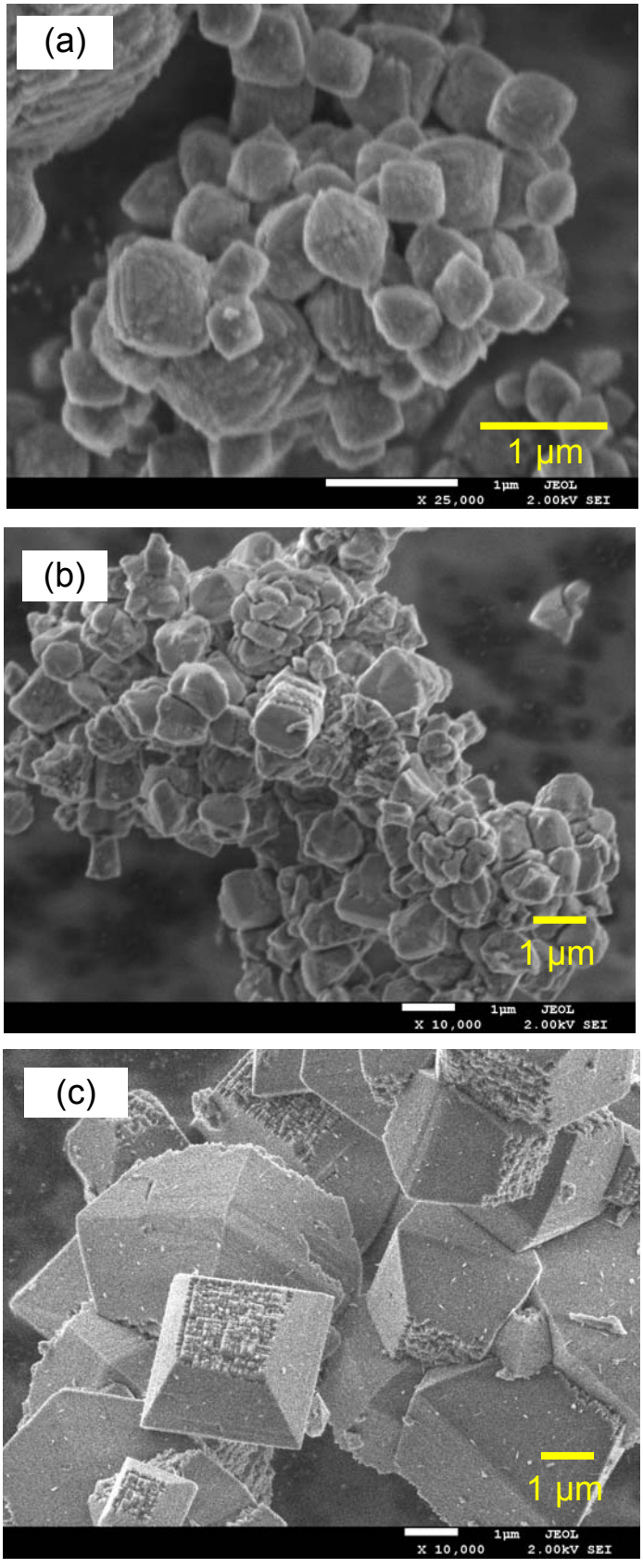

Figure S8. Typical SEM images of (a) dealuminated beta, (b) pure silica beta and (c) [Fe]-beta (Si/Fe = 58).

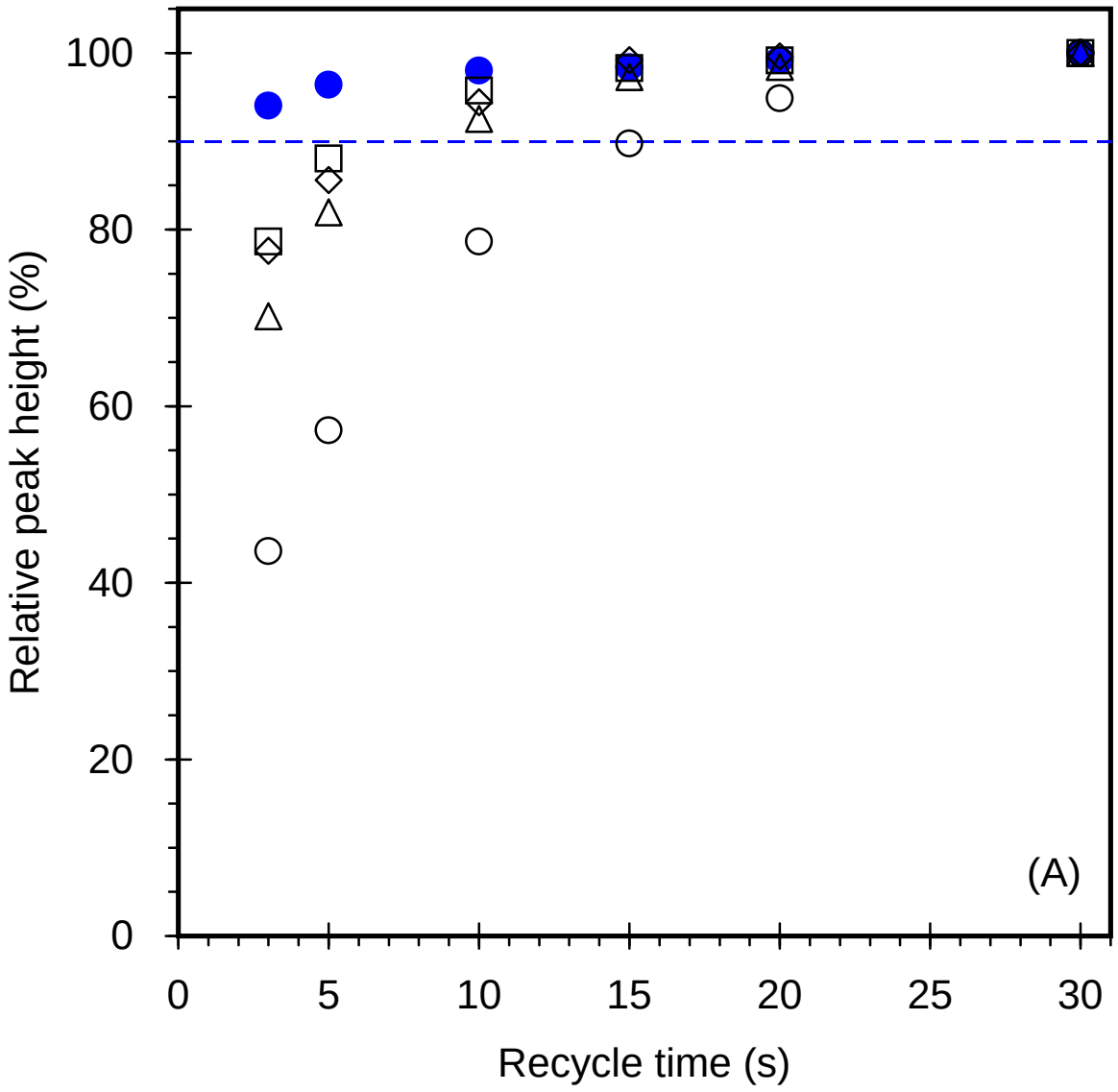

Figures S9. (A) Relative peak heights of Q^4 signals at -112 ppm by various recycle times from 3 to 30 s. (○) Unmodified deAl-beta; (△) 0.1-$Cu(NO_3)_2$/deAl-beta; (◇) 0.3-$Cu(NO_3)_2$/deAl-beta; (□) 0.5-$Cu(NO_3)_2$/deAl-beta; (●) 1.0-$Cu(NO_3)_2$/deAl-beta.

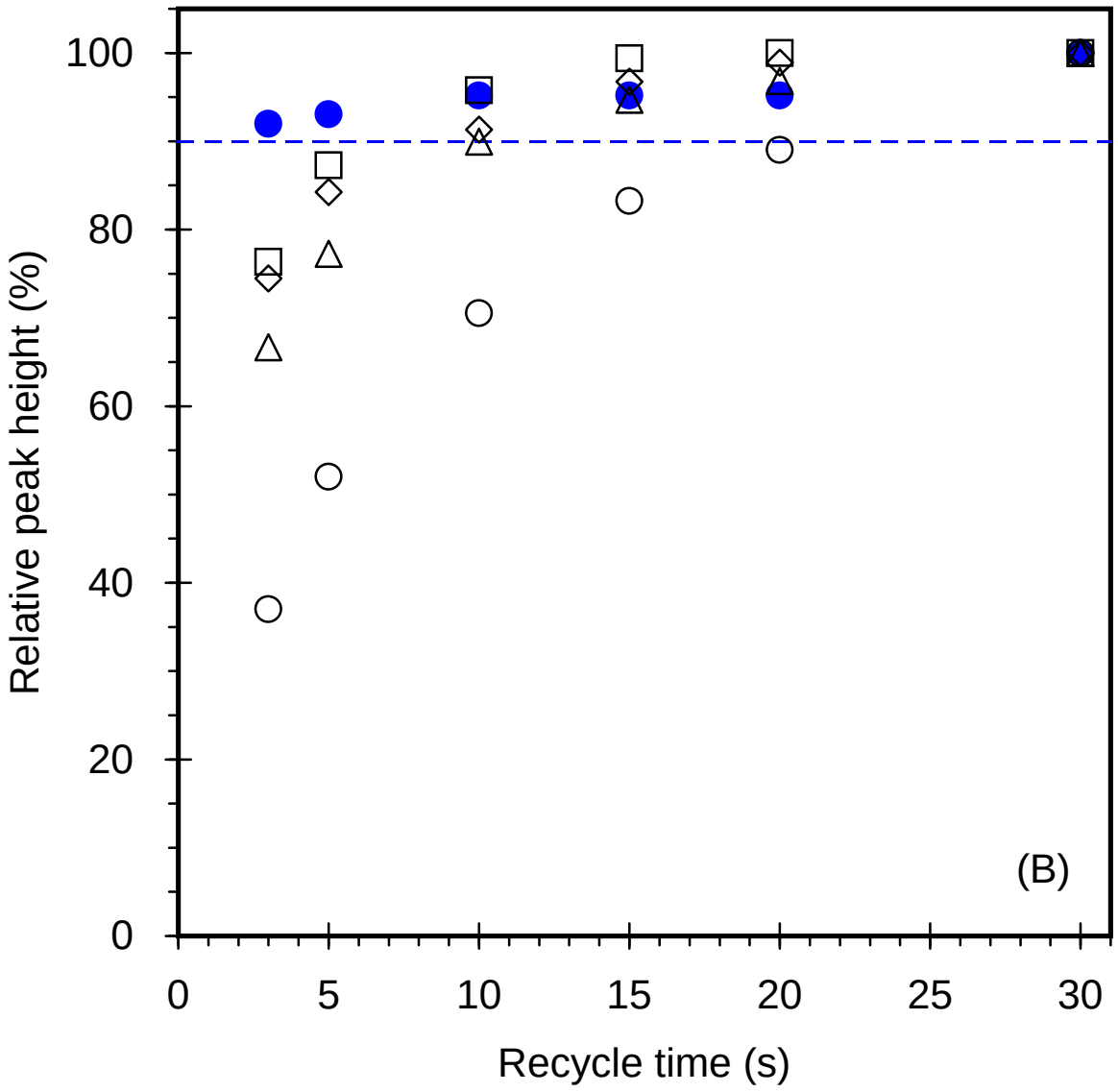

Figures S9. (B) Relative peak heights of Q^4 signals at -115 ppm by various recycle times from 3 to 30 s. (○) Unmodified deAl-beta; (△) 0.1-$Cu(NO_3)_2$/deAl-beta; (◇) 0.3-$Cu(NO_3)_2$/deAl-beta; (□) 0.5-$Cu(NO_3)_2$/deAl-beta; (●) 1.0-$Cu(NO_3)_2$/deAl-beta.

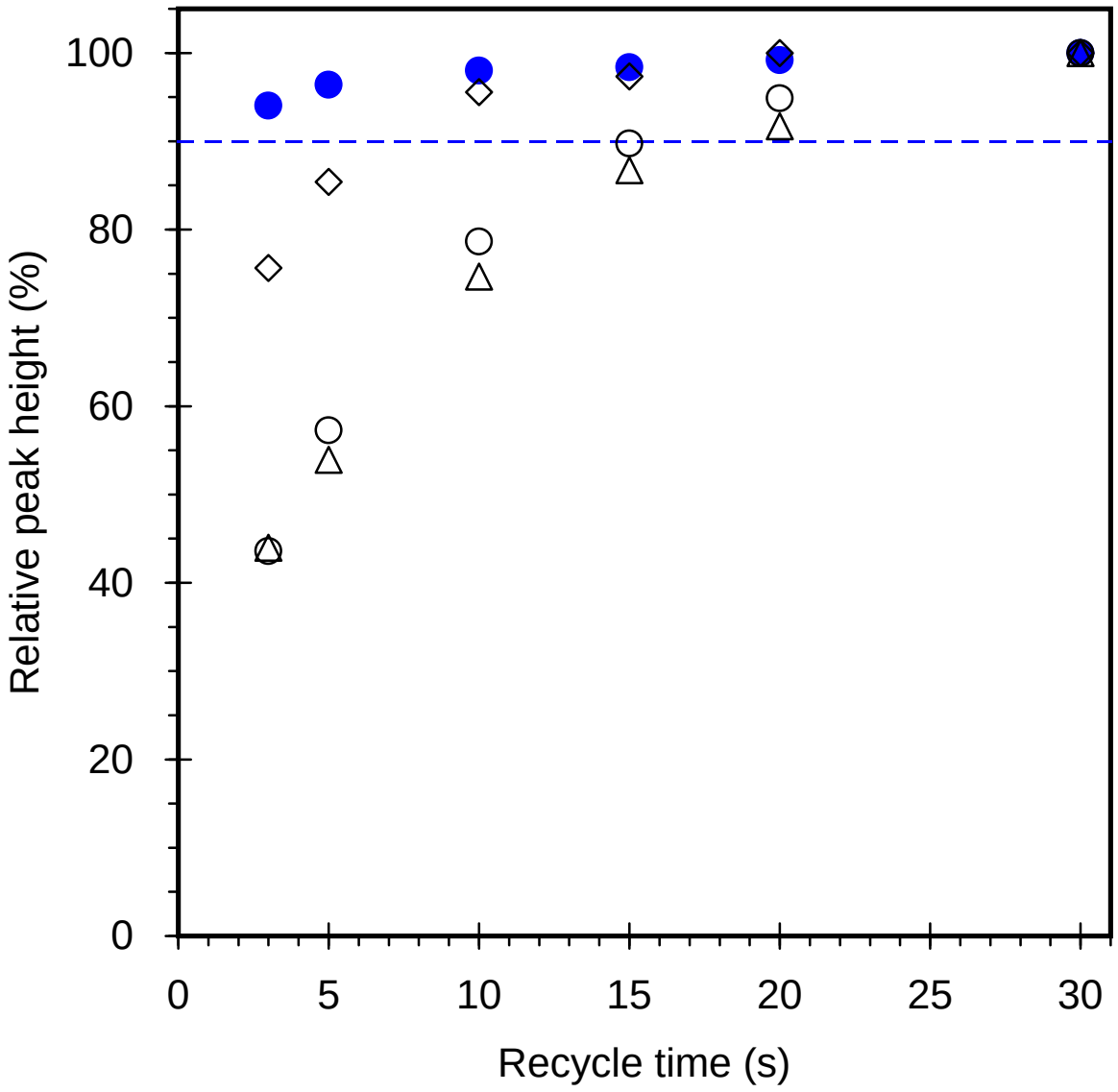

Figure S10. Relative peak heights of Q^4 signals at -112 ppm by various recycle times from 3 to 30 s. (○) Unmodified deAl-beta; (△) 1.0-$Co(NO_3)_2$/deAl-beta; (◇) 1.0-$Ni(NO_3)_2$/deAl-beta; (●) 1.0-$Cu(NO_3)_2$/deAl-beta.